Current Science International
ISSN: 2077-4435

Volume : 04 | Issue : 04 | Oct.-Dec. 2015
Pages: 621-627

Characterization of Ag Nanoparticles by Nanosecond Pulsed Laser Ablation Doped in Chitosan

[1]M. Dawy, [2]H.M. Rifaat and [3]A.A. Menazea

[1]Department of Physical, Chemistry [3]Department of Microbial Chemistry and [4]Department of spectroscopy, National Research Centre, Giza, 12622, Egypt.

ABSTRACT

Pulsed laser ablation of Ag, immersed in double-distilled water is used to synthesize Ag nanoparticles(NPs).The targets are irradiated for 10 and 30 min by laser pulses at different wavelengths the fundamental and the second harmonic (SHG) (λ = 1064 and 532 nm, respectively). The ablation process is performed at a repetition rate of 10Hz and with pulse duration of 15 ns. Two boundary values of the laser fluence for each wavelength under the experimental conditions chosen were used it varied from several J/cm^2 to tens of J/cm^2. Only as – prepared samples were measured not later than two hours after fabrication. The NPs shape and sized is attributions were evaluated from transmission electron microscopy (TEM) images. The suspensions obtained were investigated by optical transmission spectroscopy in the near UV and in the visible region in order to get information about these parameters. Spherical shape of the AgNPs at the low laser fluency and appearance of aggregation and building of nanowires at the SHG and high laser fluence was seen. Dependence of the mean particle size at the SHG on the laser fluence was established. Comments on the results obtained have been also presented. The synthesized silver nanoparticles and its composite with chitosan under different conditions: CS/Ag (L1), CS/Ag (L2), CS/Ag (L3) and CS/Ag (L4) were characterized using electron microscope SEM, TEM and UV-visible spectrophotometer. Also, visible photoluminescence (PL) emissions of the synthesized silver nano composites have been recorded. The diameters of the as-prepared nanocomposites measured were less than 20 nm. Antibacterial activities of different sizes of silver nanoparticles were investigated against Gram-positive and Gram-negative bacteria. Also, Electrical Resistivity measurements of nanocomposites showed semiconducting values (1- 4x10$^{11}\Omega$ cm**)**.

Key words: Ag Nanoparticles, Nanosecond pulsed laser ablation, Ag composites, Electrical and Antibacterial properties.

Introduction

As a result of the progress in nanotechnologies during the last two decades nowadays nanosystems find application in many areas, such as chemistry (catalysis) (Mallick *et al.*, 2006), optics(photography) (Ohko *et al.,* 2003), biology (biomarkers) (Liu *et al.,* 2008), medicine (antibacterial applications) (Murali *et al.,* 2007), and microelectronics (information storage) (Corbierre *et al.,* 2006) etc. This multilateral usage of the nanoparticles (NPs), the fundamental structures in nanotechnology, is based on the unique properties, differing considerably from those of bulk materials. Appearance of characteristic bands in the absorption spectra of metallic NPs is related to the electron gas, excited by light oscillations. For noble metals such Ag, this bands are in the visible and near UV region. The collective oscillations of electrons are sensitive to size, shape and the surrounding medium of the NPs (Yin*et al.,* 2004). The increasing of the particle size causes a red-shift of the corresponding absorption bands (Link and El-Sayed, 1999) what allows a change in size to be assessed by following the absorption. Both, silver and gold NPs have attracted intensive interest because of peculiarities of their absorption spectra in the region of the surface Plasmon resonance and the specific and very important applications in nano biotechnology. The first type is used for antibacterial protection and the second type has low toxicity and can be readily attached to molecules of biological interest (Jain *et al.,* 2007). Various methods have been used to produce AgNPs: chemical (Bell, 2003), electrochemical (Khaydarov *et al.,* 2009), photochemical (Huang *et al.,* 1996), and physical (Tien *et al.,* 2008). In the last few years pulsed laser ablation in different liquid media is one promising method for preparation of these NPs. It offers the very essential advantage for biological application to generate NPs, whose surface is not contaminated with residual ions, originating from reactants and the extremely low cost of the processing setup.

Chitosan (CS) is a biopolymer which exhibits a broad spectrum of antimicrobial and antibacterial activity by binding to the negatively charged bacterial cell wall followed by attachment to the DNA, inhibiting its replication (Kurita *et al*., 1993). For the improvement of bioactivity on chitosan, it is often combined to other bioactive materials, such as drugs. Silver (Ag) nanoparticles have high therapeutic potential and exhibit good

Corresponding Author: Magda Dawy, Department of Physical Chemistry, National Research Center, Giza, 12622, Egypt.
E-mail: m_dawy9@yahoo.com

antimicrobial activity. Ag nanoparticles have a wide range of antimicrobial activities and exhibit high performance even at a very low concentration. Ag nanoparticles have been identified to possess good potential for the treatment of cancer (Sriram, 2010). But the major disadvantage of using silver alone is that it is not specific at targeting the cancer cells and also it is toxic to the normal cells when exposed for a longer time when the size of silver used is20 nm (Vaidyanathan *et al*., 2009). CS–Ag nanocomposite is one of the rare composite materials that is seen to possess a capability of being used as a biosensor as well as in the treatment of cancer as the chitosan present in the nanocomposite is very specific to the cancer cells. It prolongs the action of silver on the affected cells while preventing the normal cell from the effect of silver. One more advantage of this nanocompositeis that it is biodegradable, i.e., it can be degraded by the enzymes present in the body making it suitable for the treatment of cancer. Apart from the treatment of cancer, the nanocomposite also possesses good antimicrobial (Sanpui *et al.,* 2008) and biosensing activity. This article represents an investigation of the size distribution and the shape of AgNPs, fabricated by pulsed laser ablation from thin plates of Ag metal, immersed in double distilled water. The product of the ablation procedure is a suspension of metal NPs, dispersed in water. The influence of the wavelength, fluence and duration of the laser irradiation on the size distribution of the AgNPs is studied. As- prepared samples are measured not later than two hours after their fabrication to avoid effects of altering the suspensions. The size distribution is obtained and the shape is estimated by TEM micrographs of the NPs and extinction spectra of the suspensions in UV/VIS regions. Also, the biological activity of the as prepared materials and electrical resistivity were measured for Ag-Chitosan nanocomposites.

Experimental:

Nd: YAG laser, which emits its fundamental line (λ) at 1064 nm and second harmonic (SH) at 532 nm producing pulsed nanosecond laser were the irradiation source. Two values of the laser fluence for each of the two wavelengths were used for Ag 5.8J/cm2 and 15.5J/cm^2 for the fundamental wavelength and 5.3J/cm^2 and 19.9J/cm^2 for the SHG, respectively. The pulse-repetition rate was 10 Hz and the pulse width was 15 ns, respectively. Silver target (diameter = 30 mm, thickness = 2 mm and 99.99% purity) was washed several times by double-distilled water and placed in an ultrasonic bath to replace the mechanical impurities. Chitosan, which considered the host material, was obtained from SIGMA – ALDRICH, USA, with molecular weight ≈ 400,000 g/mol.

Laser etching in water, with regard to laser pulse parameters, is similar to the Laser Shock Processing process (see Fig. 1 in (Mallick *et al.*, 2006), with the exception that shock is not desired, while ablation is desired. This is achieved by lowering somewhat the fluence and increasing the pulse number. The fluence is taken at the level where the material at least melts, but usually vaporizes and ionizes (plasma forms). In this section, the etching of materials up to a depth of about 1 mm by lasers with power up to some Watt and pulse duration of 10–100 ns at fluences 0.1–30 J=cm2 will be reviewed (see also Fig. 1 in Mallick *et al.*, 2006)). Fig. 1 represents various schemes of laser etching in water. In other neutral liquids, backside laser etching of transparent materials was also used (Dolgaev *et al.,* 1996a, b;Wang *et al.,* 2000).

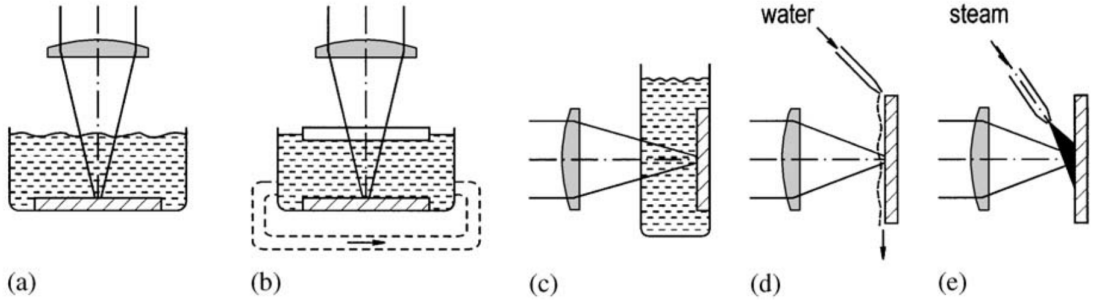

Fig. 1: Methods for providing water in the working zone during laser etching. Sources: (a) (Corbierre *et al.,* 2006); (b) (Yin *et al.,* 2004); (c)(Link and El-Sayed, 1999) ; (d) (Jain *et al.,* 2007); (e) (Corbierre *et al.,* 2006). In the cases (d) and (e), laser light not well transmitted by the water can be used. The thickness of the liquid layer over the target has typically been 1 mm:

A certain quantity of Chitosan was dissolved in double distilled water by using a magnetic stirrer at 70°C for 45 min until getting a homogenous solution of chitosan. Silver nanoparticles were produced by laser ablation of a silver target immersed into double distilled water placed at the bottom of a polypropylene vessel for the measurement and the depth of its surface was kept constant at 5mm. The vessel was slowly rotated during the ablation procedure (0.43 Hz) to avoid obvious ripples at the liquid surface and to ensure some stirring effect and

uniform ablation. The rotational velocity was kept constant and was the same during all experiments. Solutions of AgNPs and chitosan were mixed together.

The as – prepared samples were characterized by both transmission electron microscope (TEM, JEOL JEM-3010, 300 kv) and scanning electron microscope (SEM, JEOL JXA -840, Electronic Company, Japan) were used to characterize the size, dispersion of AgNPs and the morphology of CS/Ag nanocomposites. The samples for TEM were prepared by making suspension from the powder in deionized water. UV-VIS spectra of nanocomposite solution were measured using UV-VIS spectrometer (6100 Jusco, Japan).The photoluminescence (PL) emission spectra were recorded using a Perkin–Elmer LS55 fluorescence spectrophotometer in the wavelength range from 330 to 550 nm at room temperature using two excitation wavelengths kexc = 300 nm and k exc = 320 nm.. Electrical resistivity of the surface of prepared samples thin film was measured using 6517A Electrometer/High Resistance Meter. Thin films of CS/Ag nanocomposites were tested against Gram positive bacteria (*Staphyloccus aureus* and *Bacillus cereus*) and Gram negative bacteria (*Escherichia coli* and *Pseudomonas aeruginosa*) using the disk diffusion method (Bryaskova *et al.,* 2010).

Results and Discussion

Laser ablation of a solid target in a confining liquid has been demonstrated to be an effective and general route to synthesize a various range of nano crystals and nanostructures. One of the main advantages ofPulsed laser ablation of liquid PLAL is that in contrast to other methods, it produces nanoparticles free of any counter-ions or surface active substances. PLAL is a one-step, direct and very simple preparation procedure, requiring room temperature and pressure only, and therefore may be more suitable for certain commercial applications. Furthermore, as ablation takes place at the solid-liquid interface.

Probably the first experiments of laser machining under a water film were made in (Te'llez-Luis*et al.,* 2002) , with the purpose of studying the processes of material removal in interests of emission spectroscopy. Ag-nanoparticles (Ag (L1), Ag (L2), Ag (L3) and Ag (L4)) were prepared applying processes of laser etching and cutting, in the presence of liquid water at different condition as shown in table (1):

Table 1: Underwater and water-assisted laser cutting of Ag nanopaeticle condition

Sample	Power (watt)	Wave -length (nm)	Time (min)
Ag(L1)	4.6	532	10
Ag(L2)	9.6	1064	10
Ag(L3)	9.6	1064	30
Ag(L4)	4.6	532	30

TEM analysis:

The size and shape of metal nanoparticles are typically measured by analytical techniques such as TEM and SEM techniques to measure the effective size of the particles in solution. The electron micrograph of silver nanoparticles obtained by a transmission electron microscope (TEM) of Ag (L1), Ag (L2), Ag (L3) and Ag (L4) were shown in Fig.(1). This figure shows the presence of nanoparticles with an average size of 20, 19, 30 and 17 nm respectively for Silver nanoparticles Ag (L1), Ag (L2), Ag (L3) and Ag (L4) prepared by laser ablation.

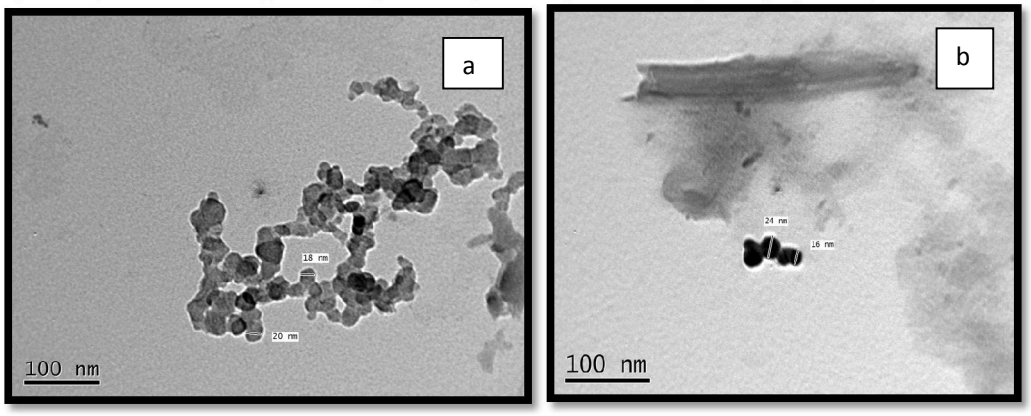

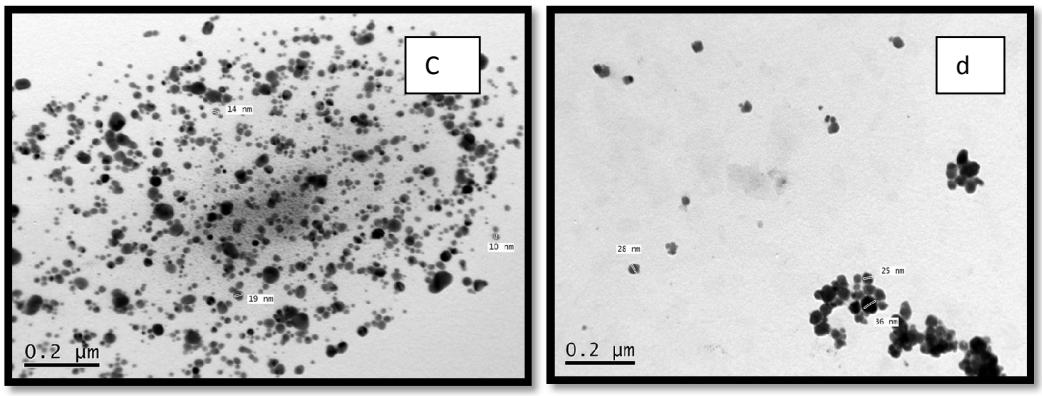

Fig . 1: TEM of (a) Ag(L1),(b) Ag(L2),(c) Ag(L3) and(d) Ag(L4)

SEM analysis:

Fig. (2). Represents surface and cross-section SEM photographs of CS/ Ag(L1),(b) CS/ Ag (L2), (c) CS/ Ag (L3) and (d) CS/Ag (L4) nanocomposites film. CS/Ag film displayed a smooth surface. SEM images of the cross- sectional surface of CS/Ag (L4) shows bright parts in the nanocomposite fractured films are the ends of the broken nanoparticles. SEM images CS/Ag (L3) and CS/Ag (L4) unsymmetric morphology; that is, the nanoparticles were dispersed throughout the chitosan matrix appeared to have intercalated morphology

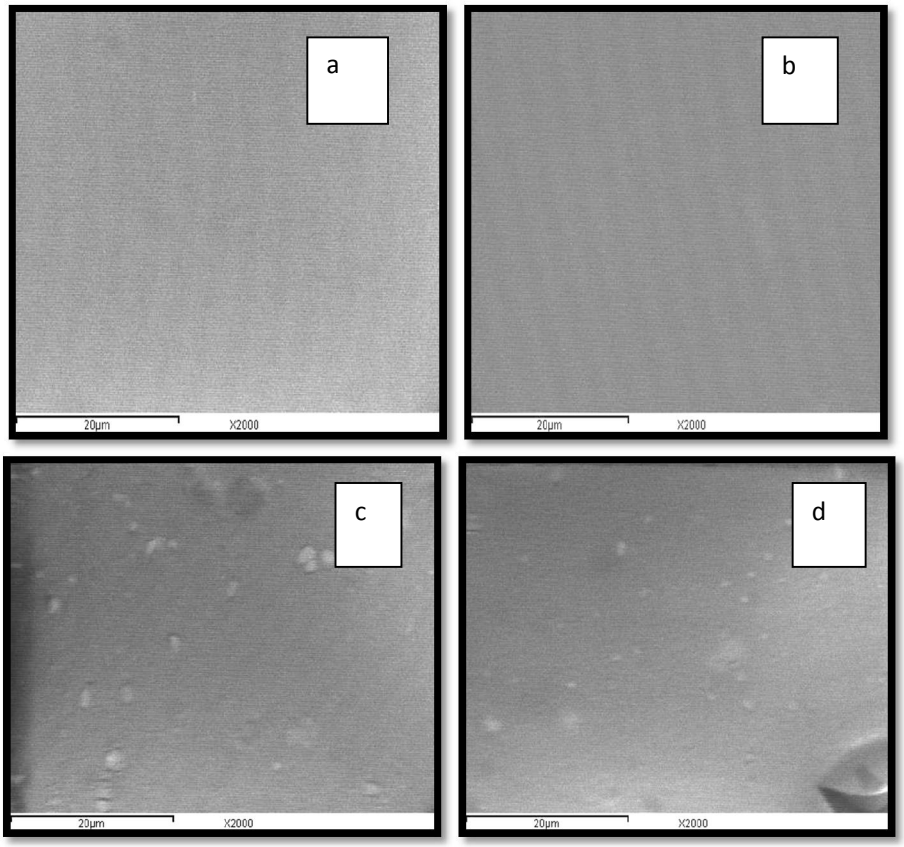

Fig. 2: SEM of (a)CS/ Ag(L1),(b) CS/ Ag(L2),(c) CS/ Ag(L3) and(d) CS/ Ag(L4)

UV-VIS spectroscopy:

Silver nanostructure exhibits interesting optical properties directly related to surface Plasmon resonance (SPR), which is highly dependent on the morphology of the samples. The spherical shape of the nanoparticles observed by TEM is consistent with the optical absorption peak around 400 nm which originates from surface-plasmon excitation.

We have measured UV-visible absorption characteristics of all the synthesized samples and those are shown in Fig. (3). It can be seen that the UV-visible absorption peaks appeared for Ag (L1), Ag(L2), Ag (L3) and Ag(L4) samples, respectively at 360, 352, 362, and 350 nm and which are close to the usual SPR wavelength of silver. The red-shift of UV-visible absorption peak in Ag (L1) and Ag (L3) samples, confirms the increase in particle size synthesized samples. On the other-hand the blue shift of UV-visible absorption peak in L3 sample confirms the increase in particle size synthesized sample. Thus UV-visible absorption analysis provides the same results as found in TEM studies. Fig3 represents absorption spectra of silver nanoparticles produced. The characteristic absorption peak around 400 nm depends strongly on the Compared the macro crystalline bandgap energy calculated for Ag (L1), Ag (L2), Ag (L3) and Ag (L4) are (2.82eV), (4.20), (2.88ev) and (2.95 eV) respectively.

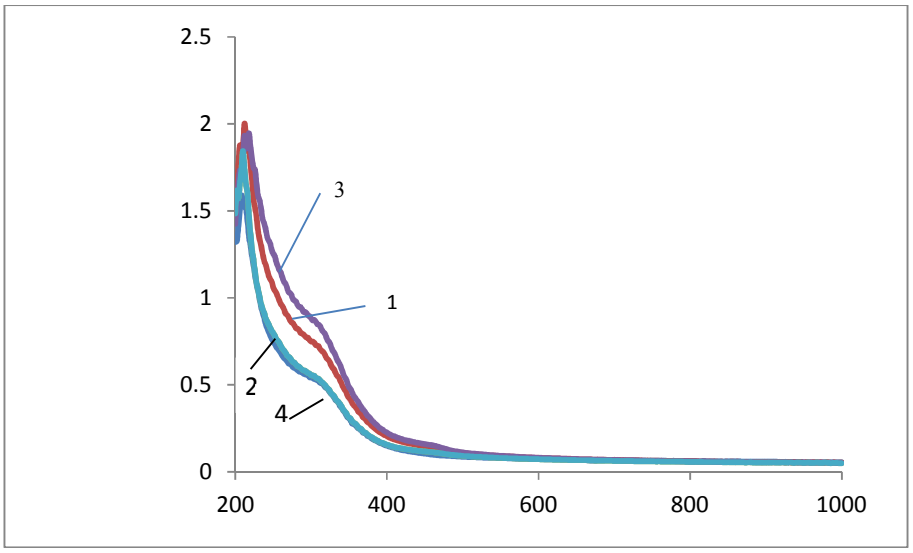

Fig. 3: UV-VIS absorption spectra of silver nanoparticles ((1) Ag (L1), (2) Ag(L2), (3) Ag (L3) and (4) Ag(L4))

Photoluminescence:

The photoluminescence emission spectra of the chitosan, for CS/Ag (L1), CS/Ag (L2), CS/Ag (L3) and CS/Ag (L4) are shown in the Fig. 4 The emission spectrum of the chitosan film is characterized by an asymmetric band with maximum emission at 410 nm, which probably originates from the protein residues in the biopolymer (Wang *et al.,* 2000). This band can be resolved by deconvolution into two sub-bands that are positioned at approximately 380 and 465 nm. The corresponding photoluminescence excitation spectrum, measured at the emission wavelength = 420 nm, showed that a maximum luminescence edge of the material should be expected for = 480 nm. After the introduction of silver in the matrix the emission is still present, but it decreases with increasing silver particle size for the nanocomposite

In addition, as the of silver particle size increases, the emission bands slightly blue shift. A possible explanation for this behavior can be drawn from an analysis of the absorption spectra of the materials. Since the silver clusters produce absorption bands in the region of chitosan emission, the observed quenching can be attributed to a non-radiative energy transfer mechanism such as charge transfer (Wang *et al.,* 2010). In the case of the nanocomposite, the observed decrease in the photoluminescence could be a consequence of the overlap between the absorption band of silver and the emission band of chitosan. Since the silver clusters produce absorption bands in the region of chitosan emission, the observed quenching can be attributed to a non-radiative energy transfer mechanism such as charge transfer (Bryaskova *et al.,* 2010). In the case of the nanocomposite, the observed decrease in the photoluminescence could be a consequence of the overlap between the absorption band of silver and the emission band of chitosan. One can expect to see the legend field transitions in these cases. However, since these transitions are Laporte forbidden, they have very low intensity. Hence, in the presence of intense charge transfer transitions one cannot detect them.

PL intensity of nanocomposites has the order: CS/Ag (L1) <CS/Ag (L3) <CS/Ag (L2) < CS/Ag (L4),It can be conceded that lowering the emission intensity, with decreasing the particle size.

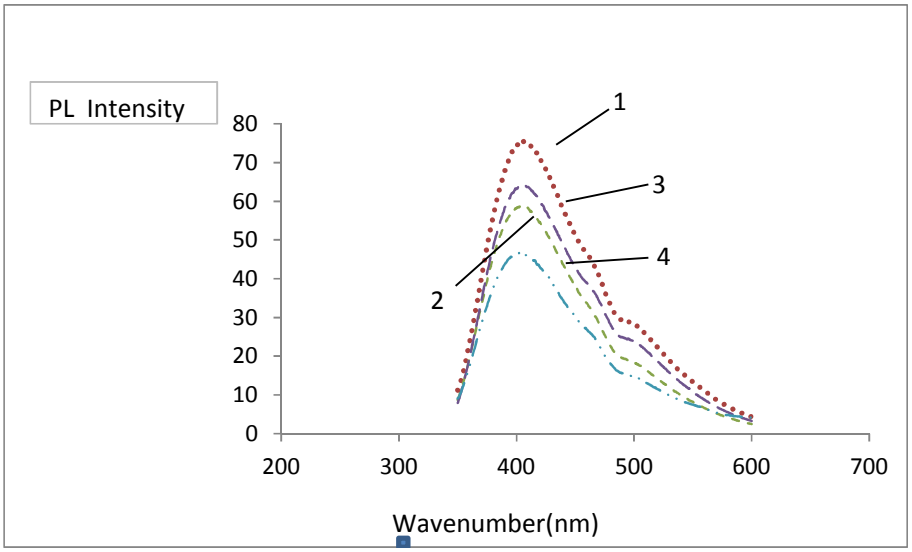

Fig. 4: UV-VIS absorption spectra of silver nanoparticles

Electrical Resistivity:

The electrical properties of CS/Ag thin film nanocomposites were studied under an applied external constant potential as a function of film thickness at metal particle size loadings. The electrical properties are directly dependent on the morphology of the silver nanoparticles embedded in the chitosan matrix.

Table 2: Electrical Resistivity, particle size and Band gap of: CS/ Ag(L1) , CS/Ag(L2), CS/Ag(L3) and CS/ Ag(L4)

Sample	Electrical Resistivity (Ω cm)	particle size (nm)
CS/ Ag L1	$4.21x10^{11}$	20
CS/ Ag L2	$1.06x10^{11}$	18
CS/ Ag L3	$1.97x10^{11}$	30
CS/ Ag L4	$2.39x10^{11}$	17

Antibacterial activity of Ag-nanocomposites:

Table (3) showed that CS/Ag (L2) and CS/Ag (L3) exhibited Antibacterialactivityagainst both Gram +ve and Gram –ve bacteria, while CS/Ag (L4) had activity only against Gram +ve bacteria. On the other hand, CS/Ag (L1) had no activity.

The synthesized silver nanoparticles and its composite with chitosan under different conditions: CS/Ag (L1), CS/Ag (L2), CS/Ag (L3) and CS/Ag (L4) were characterized using electron microscope SEM, TEM and UV-visible spectrophotometer. Also, visible photoluminescence (PL) emissions of the synthesized silver nano composites have been recorded. The diameters of the as-prepared nanocomposites measured were less than 20 nm. Antibacterial activities of different sizes of silver nanoparticles were investigated against Gram-positive and Gram-negative bacteria. Also, Electrical Resistivity measurements of nanocomposites showed semiconducting values.

Table 3: Inhibition zone of bacteria 0f CS/ Ag(L1) , CS/Ag(L2), CS/Ag(L3) and CS/ Ag(L4)

Sample	Gram +ve bacteria		Gram –ve bacteria	
	Staphylococcus aureus	*Bacillus cereus*	*Escherichia coli*	*Pseudomonas aeruginosa*
CS/Ag(L1)	0	0	0	0
CS/Ag(L2)	0	12	0	10
CS/Ag(L3)	15	15	0	12
CS/Ag(L4)	0	12	0	0

In conclusion, silver nanoparticles have been successfully generated by femtosecond pulsed laser in water. The results show that there are two kinds of particles, small particles with diameter about 17, 18 nm, and large particles with diameter about 20,30 nm, which in different time and wavelength produced by nanosecond laser ablation. The properties of the particles are characterized by SEM, TEM and UV-visible absorption spectroscopy. Antibacterial activities of different sizes of silver nanoparticles were investigated against Gram-positive and Gram-negative bacteria. Also, Electrical Resistivity measurements of nanocomposites showed semiconducting values (1- $4x10^{11}\Omega$ cm).

References

Bell, A., 2003. Science, 299: 1688-1691.
Bryaskova, R., D. Pencheva, G.M. Kale, U. Lad, T. Kantardjiev, 2010. Synthesis, characterisation and antibacterial activity of PVA/TEOS/Ag-Np hybrid thin films J. Colloid. Inter. Sci., 349: 77-85.
Corbierre, M., J. Beerens, J. Beauvais, R. Lennox, 2006. Chem. Mater., 18(11): 2628-2631.
Dolgaev, S.I., A.A. Lyalin, A.V. Simakin, G.A. Shafeev, 1996b. Fast etching of sapphire by visible range quasicw laser radiation. Appl Surf Sci., 96-98: 491-5.
Dolgaev, S.I., A.A. Lyalin, A.V. Simakin, G.A. Shafeev, 1996a. Etching of sapphire assisted by copper-vapor laser radiation. Quantum Electron., 26(1): 65-8.
Huang, H., X. Ni, G. Loy, C. Chew, K. Tan, F. Loh, J. Deng, G.Q. Xu, 1996. Langmuir., 12(4): 909-912.
Jain, P., I. El-Sayed, M. El-Sayed, 2007. Nano Today, 2(2): 18-29.
Khaydarov, R., R. Khaydarov, O. Gapurova, Y. Estrin, T. Scheper, J. NanoparYT-Res, 2009. 11: 1193-1200.
Kurita, K., K. Tomita ,T. Tada, S.L. Nishimura, S. Ishii, 1993. Reactivity characteristics of a new form of chitosan. Polym Bull., 30: 429-433.
Link, S., M. El-Sayed, J. Phys, 1999. Chem. B 103(40): 8410-8426.
Liu, X., Q. Dai, L. Austin, J. Coutts, G. Knowles, J. Zou, H. Chen, Q. Huo, J. Am, 2008. Chem. Soc., 130 (9): 2780-2782.
Mallick, K., M.J. Witcomb, M.S. Scurrell, 2006. Mater. Chem. Phys, 97: 283-287.
Murali, M.Y., K. Lee, T. Premkumar, K. Geckeler, 2007. Polymer, 48: 158-164.
Ohko, Y., T. Tatsuma, T. Fujii, K. Naoi, C. Niwa, Y. Kubota, A. Fujishima, 2003. Nat. Mater., 2: 29-31.
Sanpui, P., A. Murugadoss, P.V. Durga Prasad, S.S. Ghosh, A. Chattopadhyaya, 2008. The antibacterial properties of a novel chitosan–Ag nanoparticle composite. Int. J. Food Microbiol., 124:142-146.
Sriram M.I., 2010. Antitumor of silver nanoparticles in Dalton's lymphoma ascites tumor model. Int. J. Nanomed., 5: 753-762.
Te'llez-Luis, S.J., J.A. Ramı'rez, M. Va'zquez, 2002. J of the Science of Food and Agriculture., 82: 505-512
Tien, D.C., C.-Y. Liao, J.-C. Huang, K.-H. Tseng, J.-K. Lung, T.-T. Tsung, W.-S. Kao, T.-H. Tsai, T.-W. Cheng, B.-S. Yu, H.-M. Lin, L. Stobinski, 2008. Rev. Adv. Mater. Sci., 18: 750-756.
Vaidyanathan R., K. Kalishwaralal, S. Gopalram, S. Gurunathan, 2009. Nanosilver—the burgeoning therapeutic molecule and its green synthesis. Biotechnol. Adv., 27: 924-937.
Wang, J., H. Niino, A. Yabe, 2000. Micromachining by laser ablation of liquid: superheated liquid and phase explosion. Proc SPIE., 3933: 347–54.
Yin, Y., R. Rioux, C. Erdonmez, S. Hughes, G. Somorjai, A. Alivisatos, 2004. Science, 304: 711-714.